International Journal of Physical Medicine & Rehabilitation

Kumbhare et al., Int J Phys Med Rehabil 2014, 2:6
DOI: 10.4172/2329-9096.1000248

Research Article Open Access

Advanced Skeletal Muscle MR Imaging Approaches in the Assessment of Muscular Dystrophies

Dinesh A. Kumbhare[1,2], **Alyaa H. Elzibak**[3], **Alireza Akbari**[2] **and Michael D. Noseworthy**[2,3,4,5*]

[1]*Department of Medicine, Division of Physical Medicine and Rehabilitation, University of Toronto, Toronto, Ontario, Canada*

[2]*School of Biomedical Engineering, McMaster University, Hamilton, Ontario, Canada*

[3]*Department of Medical Physics and Applied Radiation Sciences, McMaster University, Hamilton, Ontario, Canada*

[4]*Department of Electrical & Computer Engineering, McMaster University, Hamilton, Ontario, Canada*

[5]*Department of Radiology, McMaster University, Hamilton, Ontario, Canada*

[*]**Corresponding author:** Michael D. Noseworthy, McMaster School of Biomedical Engineering, Associate Professor, Department of Electrical and Computer Engineering, McMaster University, Engineering Technology Building, ETB-406, 1280 Main St. West, Hamilton, Ontario. Canada L8S 4K1, Tel: 23727-9055259140; E-mail: nosewor@mcmaster.ca

Rec date: Aug 11, 2014; **Acc date:** Dec 16, 2014; **Pub date:** Dec 24, 2014

Abstract

Muscular dystrophies (MDs) are inherited diseases that lead to progressive skeletal muscle weakness and functional decline. Currently, the diagnosis is generally made on clinical grounds and confirmed by genetic testing, serologic assessments, neurophysiologic measurements or muscle biopsy. Given our understanding of the pathophysiology of these dystrophies, advancements in magnetic resonance imaging (MRI) techniques may assist clinicians in identification and monitoring of skeletal muscle disease progression in MDs using non-invasive approaches. In this article, we review MR imaging techniques that have been used to quantify skeletal muscle involvement in the various muscle dystrophies, such as *in vivo* spectroscopic procedures to quantify lipids (1H), muscle bioenergetics (31P) or cellular function (23Na). We also summarize studies that have used T2 relaxation measurements to evaluate muscular dystrophies. While carbon spectroscopy (13C), diffusion tensor imaging (DTI) and blood oxygenation level-dependent (BOLD) imaging have not yet been explored in the assessment of skeletal muscles of MD patients, we briefly describe these techniques as they have been useful in skeletal muscle examinations of healthy and injured muscles. Thus, they could potentially be of diagnostic and prognostic value in skeletal muscle evaluations of MD patients. The article concludes by commenting on potential for image processing methods such as texture analysis in the evaluation of muscle images from MD patients.

Keywords: MRI; Muscle; Dystrophy; T2 mapping; Spectroscopy; Diffusion tensor imaging

Introduction

Muscular dystrophies (MDs) are a number of inherited diseases that lead to skeletal muscle weakness and progressive degeneration [1]. Mutations in genes responsible for the expression of proteins essential for muscle function are behind the observed muscle wasting in MDs. The onset of these neuromuscular disorders may be at birth or early childhood, or it may not present until late into adulthood. Numerous types of MDs have been identified based on the onset age, muscles involved, and rate of muscle degeneration. Duchenne muscular dystrophy (DMD) is the most common type and is an X-linked disorder affecting mostly boys during their childhood [2]. Mutations in the dystrophin gene lead to an absence of the dystrophin cytoskeleton protein in DMD patients. Another common MD that has been linked to mutations in dystrophin is Becker muscular dystrophy (BMD). In BMD, however, dystrophin protein is not totally absent, it is present but there are alterations in its quality or amount [3]. Other MDs include myotonic muscular dystrophy (MMD), facioscapulohumeral muscular dystrophy (FSHMD), and limb-girdle muscular dystrophy (LGMD). Table 1 lists the affected muscles as well as the onset age in some of the muscle dystrophies.

In a number of these MDs, the pathophysiology is linked to the presence and function of the dystrophin protein. This creates a cascade of effects including compromised sarcolemmal structural integrity, increased intracellular calcium burden, mitochondrial dysfunction, myofibril protein degradation, apoptosis, and necrosis. Over time, these relentless effects result in the failure of the muscle degeneration/regeneration cycle due to the exhaustion of the muscle progenitor pool. Immune cell infiltration, inflammation, and connective and fatty tissue deposition displace and eventually replace the myofibers [4,5]. These processes result in skeletal muscle remodelling, heterogeneity and phenotypic plasticity [5]. In addition, the immune system plays a pivotal role; the necrotizing muscle fibres are attacked by macrophages and inflammatory cells are present throughout the skeletal muscle endomysium, perimysium, epimysium and perivascular areas [6]. Dystrophin deficiency also causes loss of sarcolemmal neuronal nitric oxide synthase (nNOSμ) and reduces paracrine signalling of muscle-derived nitric oxide (NO·) to the microvasculature, which renders the diseased muscle fibres susceptible to functional muscle ischemia during exercise. Repeated bouts of functional ischemia superimposed on muscle fibres already weakened by dystrophin deficiency results in use-dependent focal muscle injury [7]. These processes lead to progressive ultrastructural, metabolic and blood flow changes resulting in weakness and functional decline.

Although different groups of muscles may be affected in each muscle dystrophy, all MDs share common characteristics in that the

involved muscles are generally atrophied, showing fatty replacement of muscle fibres. This lipid infiltration and replacement of muscle fibres by connective tissue leads to muscle weakness and degeneration, which impacts the functional ability of MD patients. Muscle hypertrophy may also be observed. Depending on the MD type and the severity of the disease, the impairments may include minor disabilities, functional and cognitive impairments or they may be more severe leading to serious muscle damage and complete loss of life by the late twenties, as is the case of most DMD patients who die due to cardiac and respiratory failures [8].

Dystrophy	Affected Muscles	Onset Age
Duchenne	Lower limb, hips, shoulders, cardiac	Childhood (early years)
Becker	Lower limb, hips, shoulders, cardiac	5-15 years of age or adulthood
Myotonic	Facial, distal extremities	Infants to adulthood
Limb-girdle	Proximal muscles of pelvis and shoulders	Late adolescence to adulthood, sometimes childhood
Facioscapuloh umeral	Facial, upper arm, shoulder	Early adolescence, sometimes childhood

Table 1: Some Muscular Dystrophies (MDs) along with the muscles involved and the age of onset*. *A comprehensive description of other muscle dystrophies can be found in the following reference [3].

The clinical diagnosis of MDs is based on a complete physical examination and assessments of the patient's medical and family history. Laboratory tests are also conducted to evaluate serum creatine kinase (CK), an enzyme that elevates due to muscle damage. Other serologic markers that are elevated with muscle disease and that may be examined include aldolase, lactate dehydrogenase and aspartate aminotransferase. Neurophysiologic studies including nerve conduction studies and electromyography (EMG) assessments are also used to evaluate the nervous system involvement in MD sufferers. Various exercise tasks are available to examine the functional capacity of patients and functional scores are commonly employed to monitor the progression of disease. Since a genetic component is responsible for the MDs, genetic testing is used to diagnose them.

Muscle biopsies, which are generally "gold standard" approaches, suffer from sampling errors and are invasive procedures. Thus, their use may be limited in the assessment of disease status in MDs, especially because young children are commonly affected and repeated evaluations are necessary due to the tendency of muscles to degenerate over time. An imaging approach is desired in this case, as it allows for the examination of an entire muscle, or groups of muscles, and is more tolerable by young patients. Numerous imaging methods exist to evaluate skeletal muscles in the various MDs and to track disease progression including computed tomography (CT), nuclear medicine (e.g. positron emission tomography, PET and single photon emission computer tomography, SPECT), ultrasound (US) and magnetic resonance imaging (MRI). In paediatric populations the usage of nuclear medicine and CT have the disadvantage of exposing patients to ionizing radiation, even though the sensitivity and specificity are notably high (especially for PET). Furthermore nuclear medicine techniques require injection with radiotracers and have poor spatial resolution. CT scanning, although possessing superior spatial resolution, has poor soft tissue contrast, especially when compared with MRI.

Ultrasound and MRI are typically classified as non-invasive due to the lack of ionizing radiation. While US is a less expensive modality that is more accessible than MRI, it does not enable evaluations of deep muscles and is notoriously operator-dependent. This is especially problematic for quantitative studies and temporal studies that depend on consistency. It must be realized that imaging paediatric patients and obtaining high quality images is challenging, regardless of the modality used. This is because patient motion can be a problem in these young subjects who do not always comply. The use of sedation and restraint in young populations is sometimes necessary to obtain images of acceptable quality. Because of the brief list of shortcomings for imaging modalities we have focused this article on the details of MR imaging techniques that have been used in the diagnosis and prognosis of muscular dystrophies.

MR imaging approaches have shown promise in muscle assessment and recent advances have the potential to aid the clinician in evaluating MDs. Although routine anatomical MRI methods, such as T1 and T2 weighted images, are used for morphological evaluations of MDs, the focus of this article is on advanced imaging methods that enable quantitative evaluation of muscle metabolism, structure and function. These include *in vivo* spectroscopic approaches, such as proton magnetic resonance spectroscopy (1H-MRS) that allows for lipid quantification, and multinuclear spectroscopic (MNS) techniques to investigate muscle bioenergetics (31P) and cellular function (23Na). In addition, T2 mapping, which is used to gain insight into muscle composition by examining tissue proton pools, is discussed as it has been used many times to assess MDs. The article ends by summarizing MR methods that could potentially be useful in skeletal muscle evaluations in muscular dystrophies. These include *in vivo* carbon (13C) NMR spectroscopy (another MNS technique), diffusion tensor imaging (DTI) used to investigate muscle microstructure, and blood oxygenation level-dependent (BOLD) imaging that examines tissue function through local changes in the ratio of oxy to deoxyhaemoglobin. Lastly, a unique approach of evaluating MR image texture for the evaluation MD patients is presented.

Conventional Clinical MR Techniques

Standard MRI approaches that have been used to diagnose the various MDs include non-contrast T1-weighted images [9-13] and fat suppressed T2-images [14]. An MRI protocol, specific for the pediatric population, has been suggested to identify the pattern of muscle involvement for muscle dystrophies [13]. This imaging scheme is based on T1 and proton density weighted acquisitions, and is completed in less than 30 minutes [13]. The use of conventional MR imaging sequences to assess muscle dystrophies is of clinical value, however, a full discussion of routine sequences and acquisition parameter variations is beyond the scope of this review. Furthermore, numerous reviews are already available on this topic, and on the appearance of muscles of MD patients on routine clinical scans, to which we direct interested readers [15-17].

In Vivo Spectroscopic Approaches

Unlike conventional sequences, that are qualitative approaches used routinely to diagnose and monitor disease progression in muscular dystrophies, numerous quantitative spectroscopic MRI techniques are available that can provide valuable insight into biochemical properties

of skeletal muscles. The earliest documented of these *in vivo* approaches to be used in the assessment of MDs is phosphorus MRS (31P) [18]. Phosphorus studies are also the most commonly available MR spectroscopic techniques in the literature in this group of patients [18-30]. Besides 31P, evaluation of myotonic dystrophy has been carried out using sodium spectroscopy (23Na) to assess cellular physiology [31,32]. A third approach to examine muscle metabolism that is easier to perform in a clinical setting compared to the two preceding multinuclear spectroscopic techniques, is proton spectroscopy (1H). Since the majority of routine MRI examinations rely on the signals obtained from the hydrogen nucleus, clinical scanners are equipped with the hardware that is necessary to perform proton spectroscopy. Scanning of nuclei other than 1H requires unique RF coils to transmit/receive signals and a host of other specialized MR equipment (e.g. specialized RF amplifiers and T/R switches) that is not part of the standard clinical MRI package. In addition, the water peak can be used in proton spectroscopy as a reference when absolute metabolite concentrations are to be computed. However, most multinuclear approaches require the use of external references, such as tubes containing a solution of a known concentration, to act as a reference. These external solutions complicate the quantitation because they experience different magnetic field homogeneities (both B0 and B1 field) relative to the acquisition volume. Thus, MNS techniques are most commonly carried out in research-based facilities that have engineering and/or physics expertise. Surprisingly, 1H spectroscopy has only been recently used to examine lipids in skeletal muscles of MD patients [33-37], although a non-suppressed 1H spectrum from a Duchenne MD patient was presented in an early paper focusing on phosphorus imaging [18].

H Spectroscopy

A typical unsuppressed 1H spectrum from a muscle voxel of a healthy individual is dominated by a large water signal at 4.7 parts per million (ppm) and a lipid peak of smaller magnitude in the region between 1-2 ppm. Signals corresponding to trimethyl ammonium (TMA) and creatine (Cr) may also be evident in the range of 2-4 ppm, however, in order to better resolve these metabolites, water suppression is needed. The lipid signal gives information about the location of fats within the muscle cell, as this peak can be resolved into two components, one that corresponds to lipids that are found in the cytoplasm of the muscle cell, or the intra-myocellular lipids (IMCL) and another component that comes from outside of the muscle cell (extra-myocellular lipids, EMCL). Figure 1 shows an example water suppressed 1H spectrum from the anterior tibialis muscle of a healthy subject.

Since skeletal muscles are atrophied in muscular dystrophies and adipose tissue replaces muscle cells, numerous studies have demonstrated that 1H-MRS is a useful method to quantify intramuscular lipid concentrations in MD patients [33-36]. The technique has been used to investigate the lower limb muscles of Duchene sufferers [33-37]. While early studies only examined the soleus muscle of these patients [33,34], more recent investigations have included a wider group of muscles to examine disease extent among the various muscles [36]. Hsieh et al. [33,34] measured total creatine (tCr; i.e. creatine plus phosphocreatine), and TMA concentrations using proton MRS in DMD patients and healthy subjects. TMA is thought to play a role in the metabolism of phospholipids, while tCr is involved in energy metabolism. The group reported significant reductions in the TMA/tCr and TMA/water ratios in the patient population [33,34]. In addition, correlations were observed between scores of muscle function and the TMA/tCr ratio [34]. In another study, the lipid fraction in regions of interest from the soleus and tibialis anterior muscles of DMD patients was determined [35]. This value was computed by combining the concentrations of all lipid peaks between 0.9-2.3 ppm. As expected, significantly larger lipid fractions were observed in the two muscles of the DMD group when compared to healthy subjects, with the soleus muscle having a larger lipid fraction than the tibialis anterior muscle [35]. Correlations were also noted between the lipid fractions and results from tests used to assess muscle function. Lott and colleagues [36] have recently examined a larger group of DMD patients, and have evaluated four muscle compartments in the lower leg of each subject: the soleus, medial gastrocnemius, tibialis anterior and peroneal muscles. In addition, the researchers investigated the distribution of lipid metabolites by examining the IMCL and EMCL peaks. Similar to the study by Torriani et al. [35], the researchers reported that intramuscular lipid fractions in the DMD group were higher than those in the control group. In addition, dividing the DMD population into three groups based on their age (5-7 years old, 8-10 years old, and ≥ 11 years old) revealed that the older groups had larger intramuscular fat fractions [36]. With regards to EMCL and IMCL assessments, the group noted that unlike the spectra of healthy volunteers, where the lipid peak could be resolved into its two constituent signals, split resolution of the lipid peak was not always identified in the DMD group as lipid infiltration into the muscle increased [36].

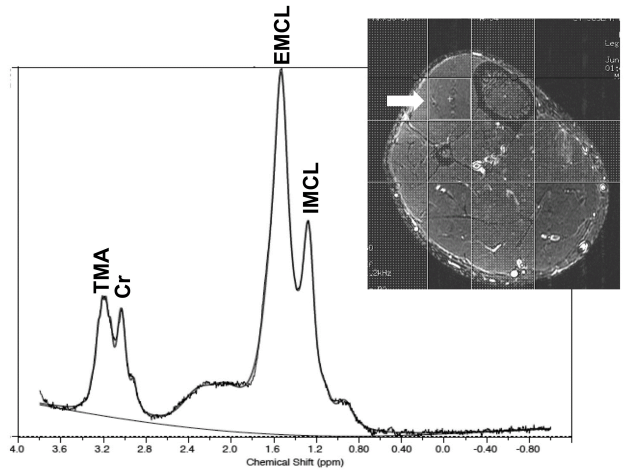

Figure 1: Sample suppressed 1H spectrum from a healthy skeletal muscle region of the anterior tibialis. Intra-myocellular (IMCL) and extra-myocellular (EMCL) lipid signals, trimethyl ammonium (TMA) and creatine (Cr) peaks are evident. Upper insert shows the axial calf slice with the location of the voxel (arrow) that was used to collect the spectrum.

For the MRS studies mentioned above (and proton spectroscopy in general), selection of the acquisition volume (voxel) is achieved most often using a point resolved spatially localized spectroscopy (PRESS) technique or infrequently with stimulated echo acquisition mode (STEAM). Both methods similarly localize a spectral volume but they differ in the RF pulses (90°-180°-180° for PRESS compared to 90°-90°-90° for STEAM). This difference results in theoretical higher

SNR for PRESS. STEAM may be of interest when the desire to minimize the effects of T2 decay as the minimum TE can be as low as ~10 ms, compared to ~30 ms for PRESS. In addition to these common methods there are numerous other spectral acquisitions, each with advantages and disadvantages, the details of which are beyond the scope of this review. Nonetheless, the acquisition of almost all 1H-MRS approaches involve careful placement of an acquisition voxel inside a muscle region of interest while attempting to minimize contributions from fat in the subcutaneous layer. The above studies demonstrate that quantification of fatty infiltration into skeletal muscles of MD patients can be carried out noninvasively and may be useful in the evaluation of disease progression. The most important caveat regarding 1H-MRS acquisition is the relationship of muscle fiber angle with respect to the main magnetic field (B0). This is often referred to as the 'magic angle effect', maximizing at 54.7°. Residual dipolar couplings change the spectral appearance of creatine, and methylene resonances of EMCLs are shifted and broadened due to bulk magnetic susceptibility (with IMCL unaffected). When muscle fibers are parallel to B0 (such as with the anterior tibialis) there is maximal separation between IMCL and EMCL. For an excellent review of this topic see Boesch et al. [38]. Further studies are needed to assess the involvement of other muscles and the clinical utility of the technique in tracking disease status.

P Spectroscopy

Since high energy phosphates (e.g. adenosine triphosphate, ATP) are the energy storage molecules in the body, non-invasive phosphorus magnetic resonance spectroscopy can be done to examine muscle bioenergetics. The technique has been used to examine energy metabolism in skeletal muscles of patients suffering from a variety of MDs [18-31,39-41] with early studies surfacing in the literature in the beginning of the 1980s, focusing on Duchenne muscular dystrophy [18]. A 31P spectrum contains dominant signals from inorganic phosphate (Pi), phosphocreatine (PCr) and three resonance signals that arise from the phosphates in ATP that are typically referred to as the α, β, and γ peaks, each progressively farther from the bulk of the molecule. Two small peaks, arising from phosphodiesters (PDE) and phosphomonoesters (PME) are also sometimes evident in a 31P spectrum of a normal resting muscle, typically only when the spectral SNR is high. Assessment of intracellular pH can be carried out from the 31P spectrum using the chemical shift difference between the Pi and PCr peaks. A sample 31P spectrum of resting calf muscle is shown in Figure 2. It should be noted that studies of dynamic spectral acquisition (e.g. spectra taking <15 seconds) are only able to resolve the dominant resonances (Pi, PCr and ATP). To visualize PMEs and PDEs temporal resolution must be sacrificed for SNR. This can be either done by increasing the acquisition volume or increasing the number of acquisition averages. The SNR increase is directly proportional to the acquisition volume and the square root of the number of averages.

Early studies using phosphorus spectroscopy to examine MDs focused on assessment of metabolite concentrations in the resting muscles, either examining forearm [18] or calf muscles [19]. Subjects suffering from numerous muscle dystrophies have been investigated using phosphorus MRS, including patients and carriers of both DMD [1-20,40] and Becker muscular dystrophy (BMD) [22,23,40]. In addition, the resting biochemical muscle properties of patients with myotonic muscular dystrophy (MMD) [24,26], limb girdle muscular dystrophy (LGMD) [25] and facioscapulohumeral muscular dystrophy (FSHMD) [29] have been assessed.

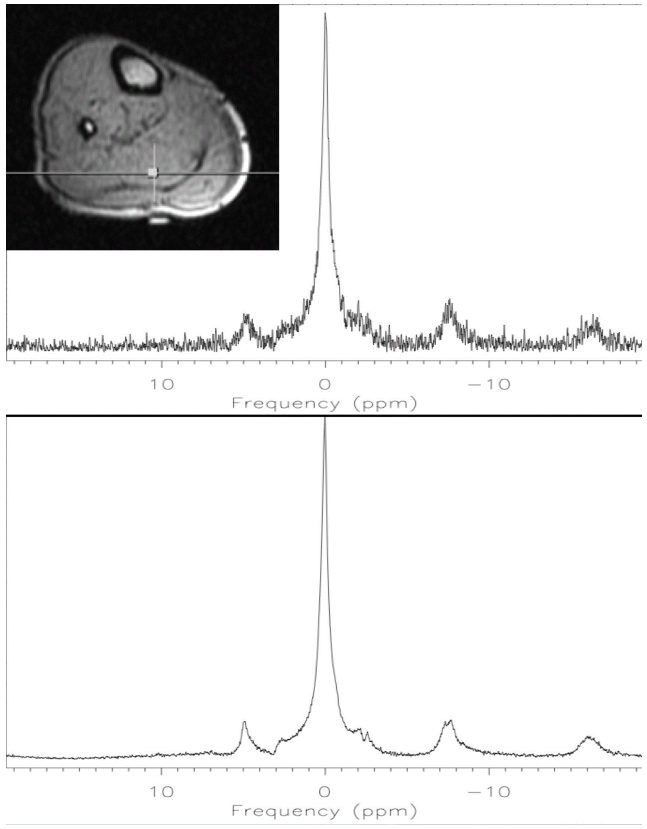

Figure 2: Upper insert shows positioning of the axial slab within the calf region, from which two phosphorus spectra were acquired. The upper 31P spectrum took twenty seconds to acquire, while the lower one took 11 minutes. Notice that longer acquisitions lead to much better peak resolution. Peaks evident are phosphocreatine (PCr at 0ppm), inorganic phosphate (Pi at 5 ppm), and adenosine triphosphate (ATP between -5 and -20 ppm).

With regards to DMD patients, impaired muscle energy metabolism has been noted, as evident from the decrease in the ratio of PCr to ATP [18,19,40] and PCr to Pi [18,19] in the resting muscle. Decreases in the ratio of PCr to ATP [23,40] and increases in the ratio of Pi to PCr [39] have also been noted in resting muscles of BMD subjects. Resting phosphorylated metabolite concentrations have been observed to be normal in the calf muscles of LGMD patients [25], while only fat infiltrated calf muscles of FSHMD patients have shown reductions in the ratio of PCr to ATP [29]. Some studies report an increase in the resting intracellular pH in the muscles of DMD [18], BMD [13,39], LGMD [25], and fat infiltrated muscles of FSHMD patients [29] compared to healthy subjects. Others, on the other hand, show no differences in the pH at rest between controls and DMD patients [19]. This is similar to resting forearm muscle assessments of myotonic dystrophy subjects that show normal intracellular pH [24, 26]. Surprisingly, evaluations of the calf muscles of these patients reveal a high pH [26]. In addition, although decreases in the ratio of PCr/ATP are observed in both the arm and calf of MMD patients, changes observed in the arm are of higher degree than those in the calf

[26]. When it comes to carriers of muscle dystrophies, phosphorylated metabolite concentrations of DMD and BMD carriers as well as non-carrier relatives of BMD patients have been shown to have similar value to those of normal subjects at rest [22,23,39].

Although examining the resting muscle using 31P spectroscopy has shown features that distinguish MD patients from those of normal subjects, phosphorus studies that evaluate metabolite concentrations both at rest, and during and following exercise, are extremely useful in gaining insight into recovery kinetics in the various muscle dystrophies [22-27,39-41]. Investigating the recovery of PCr following exercise allows for inferences to be made about mitochondrial function. Figure 3 shows a sample 31P spectrum acquired before, during and after plantar flexion exercise from the calf of a healthy subject. A reduction in PCr and an increase in Pi are observed due to the exercise.

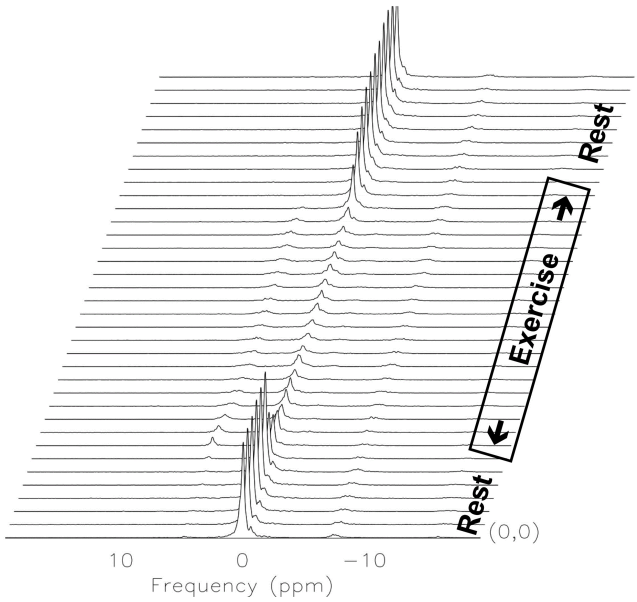

Figure 3: Sample phosphorus spectra obtained from the calf muscle of a healthy subject prior, during, and following voluntary plantar flexion at 25% maximal voluntary contraction (MVC). Notice the changes in the phosphocreatine (PCr at 0 ppm) and the inorganic phosphate (Pi at 5 ppm) peaks as a result of the exercise.

In BMD patients and gene carriers, a longer time for the pH to recover to its pre-exercise value has been reported [39]. Another study also measured a longer time for the PCr/Pi ratio to recover following isokinetic exercise in BMD/DMD carriers [22], implying abnormalities in muscle energy metabolism. Assessment of calf muscle bioenergetics following plantar flexion exercise in LGMD patients has revealed that the oxidative capacity of these patients is normal during recovery from exercise [25]. A similar finding has been observed in myotonic dystrophy patients [24] and in DMD carriers following aerobic forearm exercise [40].

Na Imaging

In myotonic muscle dystrophy, sodium channel conductance has been shown to be altered [42]. It is thus not surprising that MRS studies have utilized 23Na to non-invasively examine muscles of MMD patients [31,32]. The sodium nucleus has a spin of 3/2 and a quadrupolar moment [43]. Sodium is distributed across the cellular membrane, with a much higher concentration (approximately ten times) in the extracellular space. In biological tissues, sodium has a biexponential spin-spin (T2) relaxation time, where the short component is on the order of one millisecond [32]. The intracellular and extracellular sodium pools have been identified as originating from the 2 components of the biexponential signal decay [44-47]. Intra and extracellular sodium can also be probed using quantum filters (i.e. double and triple quantum filtering) [42,44]. Sodium imaging is challenging and requires quick data sampling schemes (pulse sequences) in order to detect the sodium signal. Figure 4 shows a sample sodium image of the calf of a healthy subject at rest. With regards to muscle dystrophies, a couple of studies have revealed that the total sodium concentration in the calf muscles of MMD patients is significantly higher than that of healthy subjects [31,32]. Correlations have also been reported between muscle sodium concentration and disease severity [31].

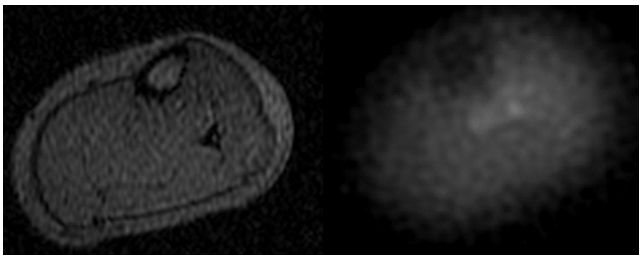

Figure 4: An axial anatomical sodium localizer (left) along with a sodium image of a healthy human calf muscle, acquired using 3 mm isotropic resolution, field of view of 18 cm, and TE/TR = 0.45/75 ms. The blurring of sodium images is due to the fast decaying sodium signal (much shorter transverse relaxation (T2)) compared to that of protons. Notice that the sodium signal is uniform in all the muscles of the healthy individual at rest.

C Spectroscopy

Although we are not aware of any studies that have used carbon spectroscopy to examine muscular dystrophies, the technique has been used to investigate skeletal muscle metabolism and it allows for the determination of glycogen levels [48-50]. However, like most multinuclear spectroscopic approaches, carbon imaging is challenging and requires additional hardware and software. For 13C spectroscopy the small carbon signal (1.1% natural abundance) needs to be boosted either through 13C enrichment, by hyperpolarization, or by proton decoupling. The most common approach is through enrichment, where, for example, a diet is given that is high in a particular 13C-labelled metabolite some time prior to the experiment [51-53]. The metabolic fate of this particular carbon then may be traced. This method is slow and researchers have more recently gravitated to hyperpolarized 13C labeled molecules that may be traced in real time following injection [54-56]. The last approach, proton decoupling, produces an increase in 13C signal through nuclear Overhauser enhancement (NOE) by destroying couplings between the low abundance carbon with that of the dominating hydrogen signal [57]. This simplifies the spectra as well because the 1H nuclei split the carbon signals into multiplets. Decoupling 1H improves the sensitivity of the acquisition such that peaks of metabolites such as glycogen can

become visible. The only downfall is a second proton RF channel is necessary, in addition to a signal waveform generator. This, along with the other challenges associated with MNS; tend to limit the wide application of the technique. A sample non-decoupled 13C spectrum from the thigh of a healthy subject is shown in Figure 5.

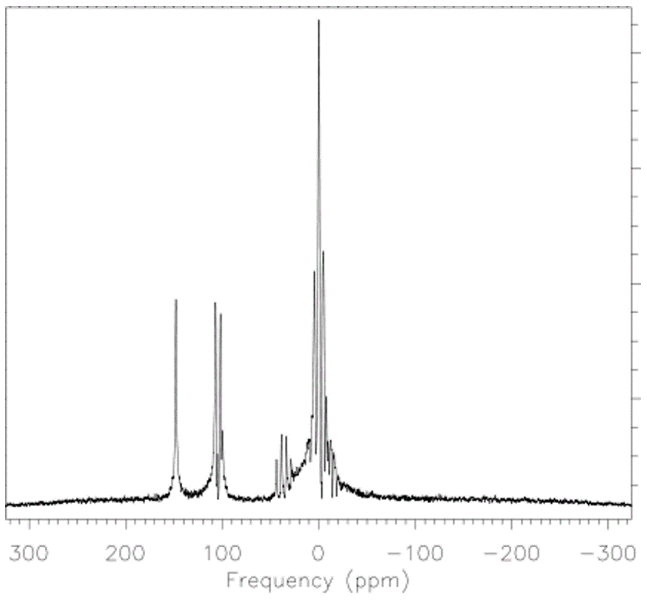

Figure 5: A sample non-decoupled 13C spectrum from the thigh muscle of a healthy subject.

Software Packages for MRS Analysis

Numerous software packages are available for the analysis of MRI spectroscopic data. Table 2 shows some of the commonly used programs for metabolite evaluations [58-60]. While some software packages are freely available, other programs have an associated cost. In addition, some packages allow for the assessment of proton spectra, while others work on both hydrogen and multinuclear elements.

Name of Program	Website	Nucleus	Supported OS	Cost
LCModel [58]	http://www.s-provencher.com/pages/lcmodel.shtml	1H,13C	Linux	≈ 15,000 US$*
jMRUI [59]/ mMRUI	http://www.mrui.uab.es/mrui/mrui_Overview.shtml	All	Linux, Windows	Free**
TARQUIN [60]	http://tarquin.sourceforge.net/index.php	1H, 13C, 31P	Windows, Linux, Mac	Free

Table 2: Software programs available for the analysis of MRI spectroscopic data. *For non-profit researchers. **Certain restrictions apply: program is free for non-commercial research uses and non-profit research organizations. Note: Website addresses were accessed on June 10th 2014.

T2 Mapping

In routine clinical scanning, the hydrogen nucleus is used to obtain images of a region of interest. This requires the use of a radio frequency (RF) pulse to excite hydrogen nuclei and allow them to oscillate. Initially, there is phase coherence in this oscillatory motion (i.e. nuclei move together). However, as the nuclei begin to return to equilibrium following termination of the RF pulse, a loss of spin phase coherence results. The relaxation mechanism that is responsible for this behaviour is referred to as the spin-spin or transverse relaxation, commonly known as T2 relaxation. This time constant thus describes the decay of the MR signal, which in a simple system and using simple imaging techniques is defined mathematically as a monoexponential decay of the form:

where Mxy is the magnitude of the transverse component of the magnetization, M0 is the initial magnetization and TE is the time at which the echo is collected. Taking the logarithm of Equation 1 and plotting the ln(Mxy) vs. TE leads to a linear fit from which the T2 time can be calculated using the slope of the straight line. Many measurements of T2 are done as described above, using a handful of TE values, each being acquired individually (ideally with the same pre-scan values for each TE).

It has been noted that the T2 time is characteristic of a tissue and can be affected by disease and physiological perturbation. T2 measurements have been used to evaluate the effects of exercise on muscles [61-64], to monitor the therapeutic responses on treatment of exercise-induced muscle injuries [65,66], and to evaluate muscle diseases [67-73]. Exercise causes changes in microvascular fluid volume, and these changes vary with the type of exercise (e.g. eccentric vs. concentric exertion) and with muscle tissue type. One common finding to all exercise studies is that T2 is noted to increase as a result of exercise. This most likely reflects the influx of water into the intracellular space by osmosis due to the movement of ions into the cell with activity [74].

Numerous studies have demonstrated the effectiveness of T2 as a reliable tool to study muscle disease [67-73]. Diseases that result in muscle physical changes involving fluctuations in vascular fluid volume and water content could be quantified through T2 measurements. With regards to muscle dystrophies, T2 investigations have been carried out in DMD patients [69,70,73,76], MMD patients [67] and FSHMD patients [75]. Higher T2 values have been reported in non-fat infiltrated regions of the anterior tibialis muscle of MMD patients compared to healthy subjects, with the highest T2 values noted with advanced disease [67]. In another study that tracked disease progression over a 2-year period in leg muscles of DMD patients, increases in T2 times were observed over the 2 years, with the older aged DMD boys showing higher progression than the younger patients [76]. In addition, correlations have been noted between T2 values in the soleus muscle and functional scores [76]. In a study that assessed thigh and pelvic muscles of DMD patients, the gluteus maximus muscle has been observed to have the highest T2 values of all the assessed muscles, and a correlation has been found between the T2 in that muscle and clinical scores [73]. T2 measurements have also been used to assess the effect of steroid treatment on the gluteus maximus muscle of DMD patients [69]. A variable response has been observed, with some patients showing increases in T2 times with

therapy, others showing no change in T2 times and a third group showing decreases in the measured T2 with therapy [69]. The increase in the T2 time was presumed to stem from an increase in fat infiltration with disease progression, while reversal of inflammation with steroids was postulated to result in reductions in the measured T2 with treatment [69]. In the group that did not show any changes in the transverse relaxation, a stable disease state has been suggested to be established with the treatment [69].

In most of the muscle dystrophy studies, no consistency is observed as to the T2 measurement: while some studies report using 2 echoes [67], others have employed 5 echoes [76], 9 echoes [69] or 11 echoes [73]. In addition, some groups use a monoexponential fit to model the signal decay [73,76], while others do not discuss the fitting algorithm [69]. There is also rarely a discussion on the T2 fit quality (i.e. R2 or $\chi 2$ values). These inconsistent T2 measurement approaches could lead to widely varying T2 values and make comparisons between different researcher groups difficult to carry out.

Although monoexponential fitting is typically employed to model the T2 decay curve, T2 in tissues is affected by the 'type' of water that is present. Compared to pure water, T2 in biological systems such as muscle is reduced by a factor of approximately 50 [77]. This fact has led to identification of at least two phases or pools of water in muscle tissue. While some researchers have attributed these pools to physical/anatomical sources, others have suggested that they are biochemical in nature [77-79]. Either way, it is accepted that exchange of water protons between these pools contributes to variations in T2 values in muscular systems.

In order to efficiently and accurately quantify the multiple fractions of T2 in muscle, many echoes are required. The individual collection of these echoes is cumbersome and time consuming. The use of a Carr-Purcell-Meiboom-Gill (CPMG) sequence, which is a modified version of Hahn's spin-echo sequence, as proposed by Carr and Purcell [80] and later improved by Meiboom and Gill [81], is the better approach when it comes to such quantitative analysis. While a single muscle T2 component (31ms) has been measured *in vivo* using 6 echoes [82], a multicomponent T2, from at least 4 water pools, has been determined in the same *in vivo* muscle study with the use of a CPMG sequence in combination with a projection presaturation technique [82]. This acquisition collected 1000 echoes from the muscle and identified four T2 components: <5 ms representing macromolecular water, 21 ± 4 ms and 39 ± 6 ms representing intracellular water, and 114 ± 31ms originating from extracellular water [82]. It is thus clear that although simple monoexponential fits are widely used to model muscle T2 decay, they do not allow for an accurate resolution of all muscular water pools. Quantitative muscle T2 is best done using a large number of echoes over a CPMG train. At least two T2 components can then be resolved, representing intracellular and extracellular/vascular pools.

Other Advanced Structural and Functional MRI Techniques

Diffusion Tensor Imaging (DTI)

Examination of muscle architecture noninvasively to gain insight into the underlying fibre structure has been carried out for over a decade using diffusion tensor imaging [83-93]. While earlier DTI studies were performed in the brain to assess the integrity of cerebral structures [94,95], the technique was quickly applied to investigate skeletal muscles due to the anisotropic muscle fibre structure. Diffusion imaging relies on the application of additional gradients to sensitize the MR signal to molecular motion. The technical detail of the imaging sequence that is used to encode diffusion and the mathematical procedure that is carried out to calculate diffusion parameters is beyond the scope of this review. Our group recently summarized these issues in a review article to which interested readers are directed [96]. A number of quantities are obtained from the diffusion measurement to describe molecular diffusion, such as the apparent diffusion coefficient (ADC), the fractional anisotropy (FA) and eigenvalues (λs) to characterize diffusion magnitude. Using the orientation of eigenvectors, tractography can be performed to visualize muscle fibre tracts. Although DTI studies have been useful in examining muscle damage and inflammatory myopathies [84,86,88], to our knowledge, the technique has not yet been applied to examine skeletal muscles of muscular dystrophy patients. A few studies do exist that assess central nervous system abnormalities in myotonic dystrophy patients using DTI [97-99]. In addition, assessment of dystrophic mouse skeletal muscle has been carried out using DTI [100]. Since myofiber abnormalities are evident in MD patients, DTI could be useful to examine muscle tissue microstructural integrity and monitor disease progression and treatment response in MD patients noninvasively.

Blood Oxygen Level-dependent (BOLD) Imaging

When functional MRI (fMRI) is mentioned, images of brain activation maps are usually assumed. Although fMRI was initially used to assess cortical responses to various stimuli, the technique has been applied to numerous other organs, including skeletal muscles [101-108] to gain insight into the microvasculature. The BOLD contrast that is exploited in fMRI studies is based on alterations in hemoglobin oxygenation such that the paramagnetic deoxyhemoglobin distorts the local magnetic field, thereby influencing the measured MR signal. Since the method uses an endogenous species as a source of contrast, it is serves as a non-invasive approach to examine muscle function. We have recently summarized the use of this technique to assess skeletal muscle microvascular environment [96]. While numerous BOLD fMRI studies have been performed to examine diseases that result in impaired perfusion to skeletal muscles [104,106,108], the method has not been used to probe skeletal muscle microcirculation in MD patients, although it has been used to examine the response of the CNS to motor stimulation in myotonic dystrophy patients [109]. Muscle degeneration is evident in the affected muscles of MD patients, and exercise intolerance is observed. However, numerous studies have not been able to find altered microcirculation in dystrophic muscles [110]. BOLD imaging might be useful to further examine microvascular status in the affected MD muscles and its noninvasive nature enables for repeated examinations to be carried out.

Image Texture Analysis

Routine clinical MR images, such as T1 and T2 weighted images, are usually visually inspected by a radiologist to qualitatively define disease extent, while quantification of spectroscopic, DTI and BOLD images usually requires more elaborate analysis techniques. Quantification of diagnostic clinical images is possible using image processing techniques such as texture analysis, which is a set of mathematical tools that enable discrimination between various regions within an image based on objective parameters such as pixel intensities

and their distribution. A number of methods are available to perform texture analysis [111] and the technique has been useful in identifying dystrophic muscles [112]. Although such approaches provide further insight into underlying image characteristics that may be difficult to discern visually, they are computationally demanding.

Summary of Mr Imaging in Muscular Dystrophies

The diagnosis of the various muscular dystrophies is carried out using standard MR techniques [9-17], including non-contrast T1-weighted images [9-13] and fat suppressed T2-images [14]. Recently, advanced MR approaches have provided valuable insight into biochemical properties of skeletal muscles of MD patients. Using 1H spectroscopy, quantifications of intramuscular lipid concentrations have been carried out in Duchene sufferers [33-37]. As expected, DMD patients show higher intramuscular lipid fractions compared to healthy controls [35,36]. The 1H spectrum gives signals from trimethyl ammonium (TMA) and total creatine (tCr), which are thought to play roles in the metabolism of phospholipids and energy metabolism, respectively. Using these signals, significant reductions in the TMA/tCr and TMA/water ratios have been noted in DMD patients compared to healthy subjects [33,34]. To better assess energy metabolism, phosphorus magnetic resonance spectroscopy (31P MRS) has been carried out on skeletal muscles of MD patients [18-31, 39-41], examining both resting muscle metabolites [18-20,22-26,40], as well as evaluating metabolite concentrations at rest, and during and following exercise to gain insight into recovery kinetics [22-27,39-41]. Impaired resting muscle energy metabolism has been noted in DMD [18,19,40], BMD [23,40], and fat infiltrated calf muscles of FSHMD patients [29]. Assessments of resting intracellular pH in the muscles of MD patients are varied. Some studies reveal increases in the resting intracellular pH in DMD [18], BMD [13,39], LGMD [25], and fat infiltrated muscles of FSHMD patients [29], while others show no differences in the pH at rest between controls and patients [19,24,26]. Using 31P spectra to investigate exercise recovery, abnormalities in energy metabolism have been observed in BMD/DMD carriers [22,39], while the oxidative capacity of LGMD [25] and MMD [24] patients has been reported to be normal during recovery from exercise. Sodium (23Na) spectroscopy has been used to assess cellular physiology non-invasively in the muscles of MMD patients, revealing significantly larger sodium concentrations in the calf muscles of patients compared to healthy controls [31,32]. It has been noted that the T2 time is characteristic of a tissue and can be affected by disease and physiological perturbation. T2 investigations have thus been carried out in DMD patients [69,70,73,76], MMD patients [67] and FSHMD patients [75]. It should be noted that no consistency is usually observed between investigators when it comes to measuring T2, with respect to the number of echoes [67, 69, 73, 76] or the fitted model used to quantify T2 [69,73,76].

Conclusions

While routine clinical MR imaging techniques are useful in the evaluation of skeletal muscle degeneration that is evident in muscle dystrophies, recent advances in MRI have led to the development of quantitative imaging methods that are of diagnostic and prognostic value. Numerous *in vivo* spectroscopic procedures are available. These can be used to quantify phosphorylated metabolites to gain insight into muscle bioenergetics (31P), to assess lipid content (1H), to examine glycogen concentration (13C), or to evaluate cellular function (23Na). T2 relaxation measurements have also shown promise in the evaluation of muscular dystrophies. While not yet explored in the assessment of skeletal muscles of MD patients, diffusion tensor imaging and blood oxygenation level-dependent imaging are emerging techniques that could potentially further our understanding of muscle architecture and microvasculature in this group of patients, respectively. Most of these advanced MR imaging approaches currently require the help of physics/ engineering personnel to ensure that they are properly implemented.

References

1. Hermans MC, Pinto YM, Merkies IS, de Die-Smulders CE, Crijns HJ, et al. (2010) Hereditary muscular dystrophies and the heart. Neuromuscul Disord 20: 479-492.
2. Bushby K, Finkel R, Birnkrant DJ, Case LE, Clemens PR, et al. (2010) Diagnosis and management of Duchenne muscular dystrophy, part 1: diagnosis, and pharmacological and psychosocial management. Lancet Neurol 9: 77-93.
3. Lovering RM, Porter NC, Bloch RJ (2005) The muscular dystrophies: from genes to therapies. Phys Ther 85: 1372-1388.
4. Blake DJ, Weir A, Newey SE, Davies KE (2002) Function and genetics of dystrophin and dystrophin-related proteins in muscle. Physiol Rev 82: 291-329.
5. Ljubicic V, Burt M, Jasmin BJ (2014) The therapeutic potential of skeletal muscle plasticity in Duchenne muscular dystrophy: phenotypic modifiers as pharmacologic targets. FASEB J 28: 548-568.
6. De Paepe B, De Bleecker JL (2013) Cytokines and chemokines as regulators of skeletal muscle inflammation: presenting the case of Duchenne muscular dystrophy. Mediators Inflamm 2013: 540370.
7. Thomas GD1 (2013) Functional muscle ischemia in Duchenne and Becker muscular dystrophy. Front Physiol 4: 381.
8. Kieny P, Chollet S, Delalande P, Le Fort M, Magot A, et al. (2013) Evolution of life expectancy of patients with Duchenne muscular dystrophy at AFM Yolaine de Kepper centre between 1981 and 2011. Ann Phys Rehabil Med 56: 443-454.
9. Mercuri E, Bushby K, Ricci E, Birchall D, Pane M, et al. (2005) Muscle MRI findings in patients with limb girdle muscular dystrophy with calpain 3 deficiency (LGMD2A) and early contractures. Neuromuscul Disord 15: 164-171.
10. Jarraya M, Quijano-Roy S, Monnier N, Béhin A, Avila-Smirnov D, et al. (2012) Whole-Body muscle MRI in a series of patients with congenital myopathy related to TPM2 gene mutations. Neuromuscul Disord 22 Suppl 2: S137-147.
11. Fischmann A, Hafner P, Gloor M, Schmid M, Klein A, et al. (2013) Quantitative MRI and loss of free ambulation in Duchenne muscular dystrophy. J Neurol 260: 969-974.
12. Degardin A, Morillon D, Lacour A, Cotten A, Vermersch P, et al. (2010) Morphologic imaging in muscular dystrophies and inflammatory myopathies. Skeletal Radiol 39: 1219-1227.
13. Mercuri E, Pichiecchio A, Counsell S, Allsop J, Cini C, et al. (2002) A short protocol for muscle MRI in children with muscular dystrophies. Eur J Paediatr Neurol 6: 305-307.
14. Kim HK, Merrow AC, Shiraj S, Wong BL, Horn PS, et al. (2013) Analysis of fatty infiltration and inflammation of the pelvic and thigh muscles in boys with Duchenne muscular dystrophy (DMD): grading of disease involvement on MR imaging and correlation with clinical assessments. Pediatr Radiol 43: 1327-1335.
15. Mercuri E, Jungbluth H, Muntoni F (2005) Muscle imaging in clinical practice: diagnostic value of muscle magnetic resonance imaging in inherited neuromuscular disorders. Curr Opin Neurol 18: 526-537.
16. Mercuri E, Pichiecchio A, Allsop J, Messina S, Pane M, et al. (2007) Muscle MRI in inherited neuromuscular disorders: past, present, and future. J Magn Reson Imaging 25: 433-440.
17. Wattjes MP, Kley RA, Fischer D (2010) Neuromuscular imaging in inherited muscle diseases. Eur Radiol 20: 2447-2460.

18. Newman RJ, Bore PJ, Chan L, Gadian DG, Styles P, et al. (1982) Nuclear magnetic resonance studies of forearm muscle in Duchenne dystrophy. Br Med J (Clin Res Ed) 284: 1072-1074.
19. Griffiths RD, Cady EB, Edwards RH, Wilkie DR (1985) Muscle energy metabolism in Duchenne dystrophy studied by 31P-NMR: controlled trials show no effect of allopurinol or ribose. Muscle Nerve 8: 760-767.
20. Younkin DP, Berman P, Sladky J, Chee C, Bank W, et al. (1987) 31P NMR studies in Duchenne muscular dystrophy: age-related metabolic changes. Neurology 37: 165-169.
21. Argov Z, Bank WJ (1991) Phosphorus magnetic resonance spectroscopy (31P MRS) in neuromuscular disorders. Ann Neurol 30: 90-97.
22. Barbiroli B, Funicello R, Ferlini A, Montagna P, Zaniol P (1992) Muscle energy metabolism in female DMD/BMD carriers: a 31P-MR spectroscopy study. Muscle Nerve 15: 344-348.
23. Hájeká M, Grosmanová A, Horská A, Urban P. (1993) Comparison of the clinical state and its changes in patients with Duchenne and Becker muscular dystrophy with results of in vivo 31P magnetic resonance spectroscopy. Eur Radiol 3:499-506.
24. Taylor DJ, Kemp GJ, Woods CG, Edwards JH, Radda GK (1993) Skeletal muscle bioenergetics in myotonic dystrophy. J Neurol Sci 116: 193-200.
25. Lodi R, Muntoni F, Taylor J, Kumar S, Sewry CA, et al. (1997) Correlative MR imaging and 31P-MR spectroscopy study in sarcoglycan deficient limb girdle muscular dystrophy. Neuromuscul Disord 7: 505-511.
26. Barnes PR, Kemp GJ, Taylor DJ, Radda GK (1997) Skeletal muscle metabolism in myotonic dystrophy A 31P magnetic resonance spectroscopy study. Brain 120 : 1699-1711.
27. Lodi R, Kemp GJ, Muntoni F, Thompson CH, Rae C, et al. (1999) Reduced cytosolic acidification during exercise suggests defective glycolytic activity in skeletal muscle of patients with Becker muscular dystrophy An in vivo 31P magnetic resonance spectroscopy study. Brain 122:121-130.
28. Schneider-Gold C, Beer M, Köstler H, Buchner S, Sandstede J, et al. (2004) Cardiac and skeletal muscle involvement in myotonic dystrophy type 2 (DM2): a quantitative 31P-MRS and MRI study. Muscle Nerve 30: 636-644.
29. Kan HE, Klomp DW, Wohlgemuth M, van Loosbroek-Wagemans I, van Engelen BG, et al. (2010) Only fat infiltrated muscles in resting lower leg of FSHD patients show disturbed energy metabolism. NMR Biomed 23: 563-568.
30. Torriani M, Townsend E, Thomas BJ, Bredella MA, Ghomi RH, et al. (2012) Lower leg muscle involvement in Duchenne muscular dystrophy: an MR imaging and spectroscopy study. Skeletal Radiol 41: 437-445.
31. Kushnir T, Knubovets T, Itzchak Y, Eliav U, Sadeh M, et al. (1997) In vivo 23Na NMR studies of myotonic dystrophy. Magn Reson Med 37: 192-196.
32. Constantinides CD, Gillen JS, Boada FE, Pomper MG, Bottomley PA (2000) Human skeletal muscle: sodium MR imaging and quantification-potential applications in exercise and disease. Radiology 216: 559-568.
33. Hsieh TJ, Wang CK, Chuang HY, Jong YJ, Li CW, et al. (2007) In vivo proton magnetic resonance spectroscopy assessment for muscle metabolism in neuromuscular diseases. J Pediatr 151: 319-321.
34. Hsieh TJ, Jaw TS, Chuang HY, Jong YJ, Liu GC, et al. (2009) Muscle metabolism in Duchenne muscular dystrophy assessed by in vivo proton magnetic resonance spectroscopy. J Comput Assist Tomogr 33: 150-154.
35. Torriani M, Townsend E, Thomas BJ, Bredella MA, Ghomi RH, et al. (2012) Lower leg muscle involvement in Duchenne muscular dystrophy: an MR imaging and spectroscopy study. Skeletal Radiol 41: 437-445.
36. Lott DJ, Forbes SC, Mathur S, Germain SA, Senesac CR, et al. (In Press) Assessment of intramuscular lipid and metabolites of the lower leg using magnetic resonance spectroscopy in boys with Duchenne muscular dystrophy. Neuromuscular Disorders. DOI: 10.1016/j.nmd.2014.03.013
37. Sharma U, Atri S, Sharma MC, Sarkar C, Jagannathan NR (2003) Skeletal muscle metabolism in Duchenne muscular dystrophy (DMD): an in-vitro proton NMR spectroscopy study. Magn Reson Imaging 21: 145-153.
38. Boesch C, Machann J, Vermathen P, Schick F (2006) Role of proton MR for the study of muscle lipid metabolism. NMR Biomed 19: 968-988.
39. Barbiroli B, Funicello R, Iotti S, Montagna P, Ferlini A, et al. (1992) 31P-NMR spectroscopy of skeletal muscle in Becker dystrophy and DMD/BMD carriers. Altered rate of phosphate transport. J Neurol Sci 109: 188-195.
40. Kemp GJ, Taylor DJ, Dunn JF, Frostick SP, Radda GK (1993) Cellular energetics of dystrophic muscle. J Neurol Sci 116: 201-206.
41. Barbiroli B, McCully KK, Iotti S, Lodi R, Zaniol P, et al. (1993) Further impairment of muscle phosphate kinetics by lengthening exercise in DMD/BMD carriers. An in vivo 31P-NMR spectroscopy study. J Neurol Sci 119: 65-73.
42. Hofmann WW, DeNardo GL (1968) Sodium flux in myotonic muscular dystrophy. Am J Physiol 214: 330-336.
43. Maudsley AA, Hilal SK (1984) Biological aspects of sodium-23 imaging. Br Med Bull 40: 165-166.
44. Jaccard G, Wimperis S, Bodenhausen G.(1986) Multiple-quantum NMR spectroscopy of S=3/2 spins in isotropic phase: a new probe for multiexponential relaxation. J Chem Phys 11: 6282-6293.
45. Bansal N, Szczepaniak L, Ternullo D, Fleckenstein JL, Malloy CR (2000) Effect of exercise on (23)Na MRI and relaxation characteristics of the human calf muscle. J Magn Reson Imaging 11: 532-538.
46. Ouwerkerk R, Bleich KB, Gillen JS, Pomper MG, Bottomley PA (2003) Tissue sodium concentration in human brain tumors as measured with 23Na MR imaging. Radiology 227: 529-537.
47. Bartha R, Menon RS (2004) Long component time constant of 23Na T*2 relaxation in healthy human brain. Magn Reson Med 52: 407-410.
48. Shulman GI, Rothman DL, Jue T, Stein P, DeFronzo RA, et al. (1990) Quantitation of muscle glycogen synthesis in normal subjects and subjects with non-insulin-dependent diabetes by 13C nuclear magnetic resonance spectroscopy. N Engl J Med 322:223-228.
49. Jehenson P, Duboc D, Bloch G, Fardeau M, Syrota A (1991) Diagnosis of muscular glycogenosis by in vivo natural abundance 13C NMR spectroscopy. Neuromuscul Disord 1: 99-101.
50. Saner M, McKinnon G, Boesiger P (1992) Glycogen detection by in vivo 13C NMR: a comparison of proton decoupling and polarization transfer. Magn Reson Med 28: 65-73.
51. Gruetter R, Adriany G, Choi IY, Henry PG, Lei H, et al. (2003) Localized in vivo 13C NMR spectroscopy of the brain. NMR Biomed 16: 313-338.
52. Ross B, Lin A, Harris K, Bhattacharya P, Schweinsburg B (2003) Clinical experience with 13C MRS in vivo. NMR Biomed 16: 358-369.
53. de Graaf RA, Mason GF, Patel AB, Behar KL, Rothman DL (2003) In vivo 1H-[13C]-NMR spectroscopy of cerebral metabolism. NMR Biomed 16: 339-357.
54. Keshari KR, Kurhanewicz J, Jeffries RE, Wilson DM, Dewar BJ, et al. (2010) Hyperpolarized (13)C spectroscopy and an NMR-compatible bioreactor system for the investigation of real-time cellular metabolism. Magn Reson Med 63: 322-329.
55. Zacharias NM, Chan HR, Sailasuta N, Ross BD, Bhattacharya P (2012) Real-time molecular imaging of tricarboxylic acid cycle metabolism in vivo by hyperpolarized 1-(13)C diethyl succinate. J Am Chem Soc 134: 934-943.
56. Day SE, Kettunen MI, Gallagher FA, Hu DE, Lerche M, et al. (2007) Detecting tumor response to treatment using hyperpolarized 13C magnetic resonance imaging and spectroscopy. Nat Med 13: 1382-1387.
57. Overhauser A (1953) Paramagnetic relaxation in metals. Phys Rev 89: 689.
58. Provencher SW1 (1993) Estimation of metabolite concentrations from localized in vivo proton NMR spectra. Magn Reson Med 30: 672-679.
59. Naressi A, Couturier C, Devos JM, Janssen M, Mangeat C, et al. (2001) Java-based graphical user interface for the MRUI quantitation package. MAGMA 12: 141-152.
60. Wilson M, Reynolds G, Kauppinen RA, Arvanitis TN, Peet AC (2011) A constrained least-squares approach to the automated quantification of in

vivo 1H magnetic resonance spectroscopy data. Magn Reson Med 65: 1-12.

61. Elliott JM, O'Leary SP, Cagnie B, Durbridge G, Danneels L, et al. (2010) Craniocervical orientation affects muscle activation when exercising the cervical extensors in healthy subjects. Arch Phys Med Rehabil 91: 1418-1422.
62. Black CD, McCully KK (2008) Force per active area and muscle injury during electrically stimulated contractions. Med Sci Sports Exerc 40: 1596-1604.
63. Black CD, McCully KK (2008) Muscle injury after repeated bouts of voluntary and electrically stimulated exercise. Med Sci Sports Exerc 40: 1605-1615.
64. Sesto ME, Chourasia AO, Block WF, Radwin RG (2008) Mechanical and magnetic resonance imaging changes following eccentric or concentric exertions. Clin Biomech (Bristol, Avon) 23: 961-968.
65. Jayaraman RC, Reid RW, Foley JM, Prior BM, Dudley GA, et al. (2004) MRI evaluation of topical heat and static stretching as therapeutic modalities for the treatment of eccentric exercise-induced muscle damage. Eur J Appl Physiol 93: 30-38.
66. Yanagisawa O, Niitsu M, Takahashi H, Goto K, Itai Y (2003) Evaluations of cooling exercised muscle with MR imaging and 31P MR spectroscopy. Med Sci Sports Exerc 35: 1517-1523.
67. Hiba B, Richard N, Hébert LJ, Coté C, Nejjari M, et al. (2012) Quantitative assessment of skeletal muscle degeneration in patients with myotonic dystrophy type 1 using MRI. J Magn Reson Imaging 35: 678-685.
68. O'Leary S, Cagnie B, Reeve A, Jull G, Elliott JM (2011) Is there altered activity of the extensor muscles in chronic mechanical neck pain? A functional magnetic resonance imaging study. Arch Phys Med Rehabil 92: 929-934.
69. Kim HK, Laor T, Horn PS, Wong B (2010) Quantitative assessment of the T2 relaxation time of the gluteus muscles in children with Duchenne muscular dystrophy: a comparative study before and after steroid treatment. Korean J Radiol 11: 304-311.
70. Mavrogeni S, Tzelepis GE, Athanasopoulos G, Maounis T, Douskou M, et al. (2005) Cardiac and sternocleidomastoid muscle involvement in Duchenne muscular dystrophy: an MRI study. Chest 127: 143-148.
71. Maillard SM, Jones R, Owens C, Pilkington C, Woo P, et al. (2004) Quantitative assessment of MRI T2 relaxation time of thigh muscles in juvenile dermatomyositis. Rheumatology (Oxford) 43: 603-608.
72. Bryan WW, Reisch JS, McDonald G, Herbelin LL, Barohn RJ, et al. (1998) Magnetic resonance imaging of muscle in amyotrophic lateral sclerosis. Neurology 51: 110-113.
73. Kim HK, Laor T, Horn PS, Racadio JM, Wong B, et al. (2010) T2 mapping in Duchenne muscular dystrophy: distribution of disease activity and correlation with clinical assessments. Radiology 255: 899-908.
74. Patten C, Meyer RA, Fleckenstein JL (2003) T2 mapping of muscle. Semin Musculoskelet Radiol 7: 297-305.
75. Kan HE, Scheenen TW, Wohlgemuth M, Klomp DW, van Loosbroek-Wagenmans I, et al. (2009) Quantitative MR imaging of individual muscle involvement in facioscapulohumeral muscular dystrophy. Neuromuscul Disord 19: 357-362.
76. Willcocks RJ, Arpan IA, Forbes SC, Lott DJ, Senesac CR, et al. (2014) Longitudinal measurements of MRI-T2 in boys with Duchenne muscular dystrophy: effects of age and disease progression. Neuromuscul Disord 24: 393-401.
77. Hazlewood CF, Chang DC, Nichols BL, Woessner DE. (1974) Nuclear magnetic resonance transverse relaxation times of water protons in skeletal muscle. Biophys J. 14:583-606.
78. Belton PS, Jackson RR, Packer KJ (1972) Pulsed NMR studies of water in striated muscle. I. Transverse nuclear spin relaxation times and freezing effects. Biochim Biophys Acta 286: 16-25.
79. Belton PS, Packer KJ (1974) Pulsed NMR studies of water in striated muscle. 3. The effects of water content. Biochim Biophys Acta 354: 305-314.
80. Carr HY, Purcell EM (1954) Effects of diffusion on free precession in nuclear magnetic resonance experiments. Phys Rev 94:630-638.
81. Meiboom S, Gill D. (1958) Modified spin-echo method for measuring nuclear relaxation times. Rev Sci Instr 29:688-691.
82. Saab G, Thompson RT, Marsh GD (1999) Multicomponent T2 relaxation of in vivo skeletal muscle. Magn Reson Med 42: 150-157.
83. Galbán CJ, Maderwald S, Uffmann K, de Greiff A, Ladd ME (2004) Diffusive sensitivity to muscle architecture: a magnetic resonance diffusion tensor imaging study of the human calf. Eur J Appl Physiol 93: 253-262.
84. Zaraiskaya T, Kumbhare D, Noseworthy MD (2006) Diffusion tensor imaging in evaluation of human skeletal muscle injury. J Magn Reson Imaging 24: 402-408.
85. Sinha S, Sinha U, Edgerton VR (2006) In vivo diffusion tensor imaging of the human calf muscle. J Magn Reson Imaging 24: 182-190.
86. Saotome T, Sekino M, Eto F, Ueno S (2006) Evaluation of diffusional anisotropy and microscopic structure in skeletal muscles using magnetic resonance. Magn Reson Imaging 24: 19-25.
87. Budzik JF, Le Thuc V, Demondion X, Morel M, Chechin D, et al. (2007) In vivo MR tractography of thigh muscles using diffusion imaging: initial results. Eur Radiol 17: 3079-3085.
88. Qi J, Olsen NJ, Price RR, Winston JA, Park JH (2008) Diffusion-weighted imaging of inflammatory myopathies: polymyositis and dermatomyositis. J Magn Reson Imaging 27: 212-217.
89. Froeling M, Oudeman J, van den Berg S, Nicolay K, Maas M, et al. (2010) Reproducibility of diffusion tensor imaging in human forearm muscles at 3.0 T in a clinical setting. Magn Reson Med 64: 1182-1190.
90. Sinha S, Sinha U (2011) Reproducibility analysis of diffusion tensor indices and fiber architecture of human calf muscles in vivo at 1.5 Tesla in neutral and plantarflexed ankle positions at rest. J Magn Reson Imaging 34: 107-119.
91. Cermak NM, Noseworthy MD, Bourgeois JM, Tarnopolsky MA, Gibala MJ (2012) Diffusion tensor MRI to assess skeletal muscle disruption following eccentric exercise. Muscle Nerve 46: 42-50.
92. Jones GE, Kumbhare DA, Harish S, Noseworthy MD (2013) Quantitative DTI assessment in human lumbar stabilization muscles at 3 T. J Comput Assist Tomogr 37: 98-104.
93. Elzibak AH, Kumbhare DA, Harish S, Noseworthy MD (2014) Diffusion tensor imaging of the normal foot at 3 T. J Comput Assist Tomogr 38: 329-334.
94. Sotak CH1 (2002) The role of diffusion tensor imaging in the evaluation of ischemic brain injury - a review. NMR Biomed 15: 561-569.
95. Beaulieu C1 (2002) The basis of anisotropic water diffusion in the nervous system - a technical review. NMR Biomed 15: 435-455.
96. Noseworthy MD, Davis AD, Elzibak AH (2010) Advanced MR imaging techniques for skeletal muscle evaluation. Semin Musculoskelet Radiol 14: 257-268.
97. Fukuda H, Horiguchi J, Ono C, Ohshita T, Takaba J, et al. (2005) Diffusion tensor imaging of cerebral white matter in patients with myotonic dystrophy. Acta Radiol 46: 104-109.
98. Ota M Sato N, Ohya Y, Aoki Y, Mizukami K, et al. (2006) Relationship between diffusion tensor imaging and brain morphology in patients with myotonic dystrophy. Neurosci Lett 407: 234-239.
99. Franc DT Muetzel RL, Robinson PR, Rodriguez CP, Dalton JC, et al. (2012) Cerebral and muscle MRI abnormalities in myotonic dystrophy. Neuromuscul Disord 22: 483-491.
100. McMillan AB Shi D, Pratt SJ, Lovering RM (2011) Diffusion tensor MRI to assess damage in healthy and dystrophic skeletal muscle after lengthening contractions. J Biomed Biotechnol 2011: 970726.
101. Noseworthy MD Bulte DP, Alfonsi J (2003) BOLD magnetic resonance imaging of skeletal muscle. Semin Musculoskelet Radiol 7: 307-315.

102. Meyer RA Towse TF, Reid RW, Jayaraman RC, Wiseman RW, et al. (2004) BOLD MRI mapping of transient hyperemia in skeletal muscle after single contractions. NMR Biomed 17: 392-398.

103. Bulte DP Alfonsi J, Bells S, Noseworthy MD (2006) Vasomodulation of skeletal muscle BOLD signal. J Magn Reson Imaging 24: 886-890.

104. Ledermann HP, Schulte AC, Heidecker HG, Aschwanden M, Jäger KA, et al. (2006) Blood oxygenation level-dependent magnetic resonance imaging of the skeletal muscle in patients with peripheral arterial occlusive disease. Circulation 113: 2929-2935.

105. Damon BM Wadington MC, Hornberger JL, Lansdown DA (2007) Absolute and relative contributions of BOLD effects to the muscle functional MRI signal intensity time course: effect of exercise intensity. Magn Reson Med 58: 335-345.

106. Schulte AC Aschwanden M, Bilecen D (2008) Calf muscles at blood oxygen level-dependent MR imaging: aging effects at postocclusive reactive hyperemia. Radiology 247: 482-489.

107. Towse TF Slade JM, Ambrose JA, DeLano MC, Meyer RA (2011) Quantitative analysis of the postcontractile blood-oxygenation-level-dependent (BOLD) effect in skeletal muscle. J Appl Physiol (1985) 111: 27-39.

108. Jacobi B, Schulte AC, Partovi S, Michel S, Karimi S, et al. (2013) Alterations of skeletal muscle microcirculation detected by blood oxygenation level-dependent mri in a patient with granulomatosis with polyangiitis. Rheumatology 52:579-581.

109. Caramia F Mainero C, Gragnani F, Tinelli E, Fiorelli M, et al. (2010) Functional MRI changes in the central motor system in myotonic dystrophy type 1. Magn Reson Imaging 28: 226-234.

110. Lombard JH (2011) Microcirculation in a mouse model of Duchenne muscular dystrophy: another blow to the vascular hypothesis? J Appl Physiol (1985) 110: 587-588.

111. Castellano G Bonilha L, Li LM, Cendes F (2004) Texture analysis of medical images. Clin Radiol 59: 1061-1069.

112. Herlidou S Rolland Y, Bansard JY, Le Rumeur E, de Certaines JD (1999) Comparison of automated and visual texture analysis in MRI: characterization of normal and diseased skeletal muscle. Magn Reson Imaging 17: 1393-1397.